

CdSe and CdSe/CdS Nanorod Solids

Dmitri V. Talapin,^{*,†,‡} Elena V. Shevchenko,^{†,§} Christopher B. Murray,[‡]
Andreas Kornowski,[†] Stephan Förster,[†] and Horst Weller[†]*Contribution from the Institute of Physical Chemistry, University of Hamburg, Grindelallee 117,
20146 Hamburg, Germany, and IBM T. J. Watson Research Center, 1101 Kitchawan Road,
Yorktown Heights, New York 10598*

Received June 3, 2004; E-mail: dmitrit@us.ibm.com; talapin@chemie.uni-hamburg.de

Abstract: We demonstrate the self-organization of CdSe nanorods into nematic, smectic, and crystalline solids. Layered colloidal crystals of CdSe nanorods grow by slow destabilization of a nanocrystal solution upon allowing the diffusion of a nonsolvent into the colloidal solution of nanocrystals. The colloidal crystals of nanorods show characteristic birefringence, which we assign to specific spherulite-like texture of each nanorod assembly. To demonstrate the general character of nanorod self-assembly technique, CdSe/CdS heterostructure nanorods were organized into highly luminescent superlattices.

Introduction

Colloidal nanocrystals (also referred to as “quantum dots”) have received steadily growing interest because of fascinating properties substantially different from the bulk materials.¹ Recent progress in the colloidal synthesis allows preparation of highly crystalline and monodisperse nanocrystals with controllable particle sizes and shapes.^{2–4} The possibility of designing the electronic structure inside each nanocrystal, e.g., formation of the type I and type II heterostructures,⁵ makes these materials attractive building blocks of nanoelectronic devices.

Assembly of functional nanosized building blocks into macroscopic superstructures is the important prerequisite for electronic and optoelectronic applications of nanocrystals. Various techniques to organize metal and semiconductor nanocrystals have been pursued for more than a decade.^{6,7} Colloidal self-assembly attracts special attention because this method allows easy formation of 3D ordered structures from building blocks that are too small to be produced by existing lithographic “top down” approaches.⁸ Recently, considerable progress in the preparation of self-assembled ordered structures from spherical noble metal,⁹ semiconductor,^{3,10,11} and magnetic^{12,13} nanocrystals

has been achieved. Moreover, the growth of complex structures from spherical nanocrystals of two different sizes^{13,14} and different functionalities (e.g., magnetic and semiconductor ones) has been demonstrated.¹⁵ Progress in chemical synthesis now allows precise control of not only a nanocrystals size but also its shape (e.g., rod, disk, etc).^{2,4} Onsager’s theory¹⁶ as well as extensive computer simulations^{17–19} predict formation of a series of orientationally and/or positionally ordered phases upon assembly of anisotropic particles. These theoretical predictions were successfully verified for micrometer-size rodlike particles of β -FeOOH and tobacco mosaic virus.^{20,21} However, the applicability of the existing theories to the nanoscale objects is questionable because we have almost no quantitative information about the interplay among van der Waals forces, thermal energy, and the other forces affecting nanoparticle dispersions. Moreover, only limited progress has been made in organizing nanocrystals with significant shape anisotropy.^{22–24}

In this contribution, we report for the first time the techniques that induce the organization of nanorod building blocks into 3D solids with a choice of glassy, nematic, smectic, or crystalline ordering. We demonstrate the generality of the assembly methods

[†] University of Hamburg.[‡] IBM T. J. Watson Research Center.[§] Current address: Department of Applied Physics and Applied Mathematics, Columbia University, New York, NY 10027.

- (1) Alivisatos, A. P. *Science* **1996**, *271*, 933.
- (2) Peng, X.; Manna, L.; Yang, W. D.; Wickham, J.; Scher, E.; Kadavanich, A.; Alivisatos, A. P. *Nature* **2000**, *404*, 59.
- (3) Murray, C. B.; Kagan, C. R.; Bawendi, M. G. *Annu. Rev. Mater. Sci.* **2000**, *30*, 545.
- (4) Kim, F.; Song, J.; Yang, P. *J. Am. Chem. Soc.* **2002**, *124*, 14316.
- (5) Weller, H. *Adv. Mater.* **1993**, *5*, 88.
- (6) Schmid, G.; Talapin, D. V.; Shevchenko, E. V. *Self-Assembly of Metal Nanoparticles. In Nanoparticles: From Theory to Applications*; Schmid, G., Ed.; Wiley-VCH: Weinheim, Germany, 2004; pp 251–304.
- (7) Alivisatos, A. P.; Peng, X.; Wilson, T. E.; Johnsson, K. P.; Loweth, C. J.; Bruchez, M. P., Jr.; Schultz, P. G. *Nature* **1996**, *382*, 609.
- (8) Rogach, A. L.; Talapin, D. V.; Shevchenko, E. V.; Kornowski, A.; Haase, M.; Weller, H. *Adv. Funct. Mater.* **2002**, *12*, 653.
- (9) Korgel, B. A.; Zaccheroni, N.; Fitzmaurice, D. *J. Am. Chem. Soc.* **1999**, *121*, 3533.
- (10) Murray, C. B.; Kagan, C. R.; Bawendi, M. G. *Science* **1995**, *270*, 1335.

- (11) Talapin, D. V.; Shevchenko, E. V.; Kornowski, A.; Gaponik, N.; Haase, M.; Rogach, A. L.; Weller, H. *Adv. Mater.* **2001**, *13*, 1868.
- (12) Sun, S.; Murray, C. B.; Weller, D.; Folks, L.; Moser, A. *Science* **2000**, *287*, 1989.
- (13) Shevchenko, E. V.; Talapin, D. V.; Rogach, A. L.; Kornowski, A.; Haase, M.; Weller, H. *J. Am. Chem. Soc.* **2002**, *124*, 11480.
- (14) Kiely, C. J.; Fink, J.; Brust, M.; Bethell, D.; Schiffrin, D. J. *Nature* **1998**, *396*, 444.
- (15) Redl, F. X.; Cho, K.-S.; Murray, C. B.; O’Brien, S. *Nature* **2003**, *423*, 968.
- (16) Onsager, L. *Ann. N.Y. Acad. Sci.* **1949**, *51*, 627.
- (17) Frenkel, D.; Lekkerkerker, H. N. W.; Stroobants, A. *Nature* **1988**, *332*, 822.
- (18) Schilling, T.; Frenkel, D. *Phys. Rev. Lett.* **2004**, *92*, 085505.
- (19) McGrother, S. C.; Williamson, D. C.; Jackson, G. *J. Chem. Phys.* **1996**, *104*, 6755.
- (20) Maeda, H.; Maeda, Y. *Phys. Rev. Lett.* **2003**, *90*, 018303.
- (21) Wen, X.; Meyer, R. B.; Caspar, D. L. D. *Phys. Rev. Lett.* **1989**, *63*, 2760.
- (22) Li, L.-s.; Alivisatos, A. P. *Adv. Mater.* **2003**, *15*, 408.
- (23) Kim, F.; Kwan, S.; Akana, J.; Yang, P. *J. Am. Chem. Soc.* **2001**, *123*, 4360.
- (24) Nikoobakht, B.; Wang, Z. L.; El-Sayed, M. A. *J. Phys. Chem. B* **2000**, *104*, 8635.

by utilizing CdSe nanorods of a variety of diameters and lengths as well as employing highly luminescent CdSe/CdS nanorod heterostructures.²⁵ Both these materials exhibit anisotropic optical properties^{25,26} attractive for optoelectronic applications.

Experimental Section

Synthesis of CdSe and CdSe/CdS Nanorods. Wurtzite CdSe nanorods with an elongated *c*-axis were synthesized according to modified literature methods.²⁷ The narrowest distribution of nanorod sizes and aspect ratios is observed when we use *n*-octadecylphosphonic acid instead of *n*-tetradecylphosphonic acid used previously in ref 27. The length of nanorods is varied from 10 to 40 nm, while their diameter is adjusted between 3 and 5 nm, thus allowing aspect ratios from 2 up to above 10 to be studied. Colloidal CdSe/CdS heterostructure nanorods were prepared as described in ref 25.

Self-Assembly of CdSe Nanorods on a TEM Grid. Four hundred mesh carbon-coated copper grids were pretreated by dipping in toluene for 20 s. After this treatment, the grids were placed inside 2-mL vials containing $\sim 2 \mu\text{L}$ of colloidal solution. We used either toluene or toluene–butyl ether (3:1) mixtures as the solvent. The solvent was evaporated either under ambient conditions (toluene) or under reduced pressure at 40–60 °C (toluene–butyl ether). Drying of the colloidal solution led to the formation of thin films on both TEM grids and walls of the vial. The grids were detached from the vial wall and investigated by TEM. We found that adding a small amount of hexadecylamine to the solution of CdSe nanorods in toluene increased the probability of the CdSe nanorods packing perpendicular to the surface of the TEM grid. Different nanorod concentrations were tested. The use of relatively concentrated solutions resulted in well-ordered nanorod assemblies, whereas the use of dilute solutions did not favor the formation of ordered superlattices.

Growing the Colloidal Crystals. In a typical experiment, we filled a glass tube of 15 cm in length and 0.8 cm in diameter with $\sim 2 \text{ mL}$ of colloidal solution of nanorods in toluene ($\sim 5 \text{ mg/mL}$). The layer of 2-propanol mixed with methanol (1:1 by volume, $\sim 3 \text{ mL}$) was carefully added above the solution of nanorods as shown in Figure 1a. The tube was sealed and left in the dark for 1–2 weeks. During this time, the nanorod superstructures nucleated and grew on the walls of the tube. The nanorod assemblies formed needed to be detached from the walls for further investigation. Detaching them from the walls could damage brittle assemblies, and to avoid this we inserted a plate of glass or ITO-coated glass into each tube, as is shown in Figure 1a. After completing the experiment, the plates were taken out of the tube, washed with methanol, and investigated by optical microscopy, SEM, and high-resolution SEM (HRSEM).

Sample Characterization. Transmission electron microscopy (TEM) and energy-dispersive X-ray analysis (EDX) were performed on Philips CM-12 and Philips CM-300 microscopes. SEM and HRSEM investigations were carried out using the LEO 1550 scanning electron microscope with a spatial resolution of 1 nm. For optical characterization, we used Zeiss Axiovert S 100 light microscope equipped with a Zeiss AxioCam CCD camera. Colloidal solutions of CdSe and CdSe/CdS nanorods were characterized by UV–vis absorption (Cary 50 UV–vis spectrometer, Varian) and photoluminescence (FluoroMax-2 spectrofluorimeter, Instruments SA).

Results and Discussion

The conventional approaches to assemble colloidal nanoparticles are based on gentle evaporation of a colloidal solution of

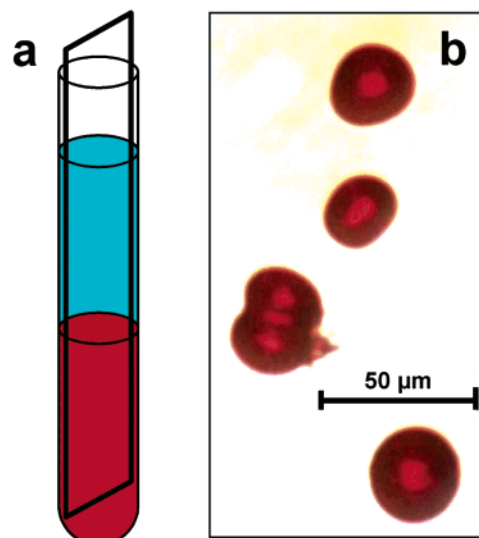


Figure 1. (a) Scheme illustrating the oversaturation technique used for crystallization of nanorods. Red: colloidal solution nanorods in toluene; blue: the layer of nonsolvent (1:1 by volume mixture of methanol and 2-propanol). The glass plate was placed inside the tube as a substrate for growing nanorod superstructures. (b) Optical micrograph of self-assembled aggregates consisting of 18 nm \times 3 nm CdSe nanorods.

nanocrystals. Monodisperse spherical CdSe nanocrystals form under these conditions long-range ordered superlattices.^{3,8} This ordering process is entropy-driven and goes toward the highest packing density. The phenomenon of entropically driven assembly in a colloidal solution is based on a rather counterintuitive fact that an *ordered* arrangement of colloidal particles can *increase* the total entropy of the system by increasing the entropy of solvent molecules.²⁸ Self-assembly of rods is less entropically favorable because it requires both positional and orientational ordering of individual rods. Recent computer simulations predict stunted crystal growth in ensembles of hard spherocylinders because of kinetic “self-poisoning” of lamellar crystal nuclei.¹⁸ As a result, nanorod assemblies with long-range order have proven to be difficult to produce. Conditions appropriate for self-assembly of spherical nanocrystals have led to disordered or locally ordered assemblies with nanorods aligned parallel to a substrate.²² Upon slow concentrating of a colloidal solution, nematic or smectic-A ordering has been observed for single layers of CdSe and BaCrO₄ nanorods.^{22,23} In these phases, the nanorods on average have a common orientation (director) but with either no positional order or only partial positional order of the individual nanorods. Films of CdSe and BaCrO₄ nanorods thicker than one monolayer showed only nematic ordering.^{22,23} We found that evaporating toluene solutions of monodisperse CdSe nanorods leads only to the formation of solids with nematic order (Figure S1 from Supporting Information). However, if a high boiling solvent such as butyl ether is added to the concentrated nanorod solution followed by drying at 40–60 °C under reduced pressure, long tracks of CdSe nanorods stacked side by side are formed (Figure 2a). At higher concentrations, these tracks align parallel to each other, resulting in smectic-A ordered superstructures (Figure 2b).

The attractive dipolar interactions between adjacent nanorods might be the driving force for formation of nanorod tracks. CdSe

(25) Talapin, D. V.; Koeppe, R.; Götzinger, S.; Kornowski, A.; Lupton, J. M.; Rogach, A. L.; Benson, O.; Feldmann, J.; Weller, H. *Nano Lett.* **2003**, *3*, 1677.

(26) Hu, J.; Li, L.-s.; Yang, W.; Manna, L.; Wang, L.-w.; Alivisatos, A. P. *Science* **2001**, *292*, 2060.

(27) Manna, L.; Scher, E. C.; Li, L.-s.; Alivisatos, A. P. *J. Am. Chem. Soc.* **2002**, *124*, 7136.

(28) Safran, S. A.; Clark, N. A. *Physics of Complex and Supramolecular Fluids*; Wiley: New York, 1987.

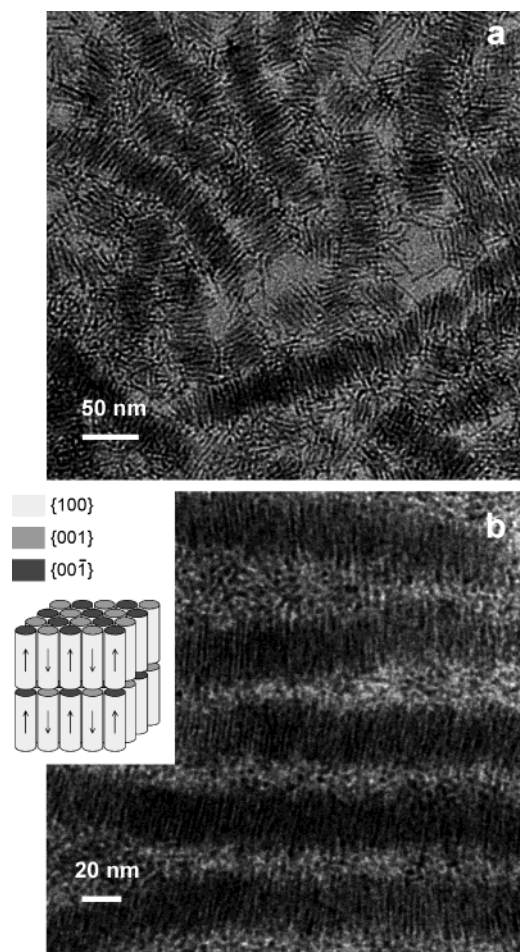


Figure 2. TEM images of CdSe nanorods self-assembled in (a) tracks and (b) superstructures with smectic-A ordering. Inset to frame (b) shows a possible orientation of CdSe nanorods allowing energetically favorable antiparallel pairing of dipole moments of individual nanorods.

noncentrosymmetric (wurtzite) crystallographic lattice causes the large permanent dipole moment along the long axis of the nanorod.²⁹ Simulations predict that the assembly of long rods into a smectic-A ordered phase can be an entropy-driven process.¹⁷ However, we believe that the formation of separated tracks of CdSe nanorods (Figure 2a) points to the important role of the electrostatic forces in self-assembly of CdSe nanorods. Pairing of the dipole moments could be responsible for the formation and thermodynamic stability of nanorod superstructures. Monte Carlo simulations for hard spherocylinders show that longitudinal dipoles can stabilize the layered smectic phases due to antiparallel side-by-side dipole pairing within a layer and between the adjacent layers (Figure 2b, inset).³⁰ In fact, antiparallel pairing of magnetic dipoles induced the formation of similar tracks of Co nanorods.³¹

We have developed a technique for growing macroscopic nanorod superlattices by destabilization of a colloidal solution upon slow molecular diffusion of a nonsolvent (methanol/2-propanol 1:1 mixture) into a toluene dispersion of nanorods (Figure 1a). A similar approach has been employed to grow perfectly faceted colloidal crystals from monodisperse spherical

CdSe,¹¹ FePt,³² and CoPt₃.¹³ In contrast to the conventional evaporation-based techniques, molecular diffusion of a nonsolvent avoids the development of temperature gradients and local flows in solution.

Diffusion of methanol/2-propanol mixture into a solution of CdSe nanorods dispersed in toluene with 0.1% hexadecylamine induces nucleation and growth of the nanorod superstructures on the walls of the tube and on the surface of the inserted glass plate (Figure 1a).

Figure 1b shows a typical optical photograph of 18 nm × 3 nm CdSe nanorods self-assembled on a glass surface. Similar platelet-like assemblies were also found on walls of the tube. Figure 3a shows a representative SEM image of one nanorod assembly. Gentle sonication in 2-propanol removes the assemblies from the substrate and cleaves them into flat sheets shown in Figure 3b,c. HRSEM images taken directly from the edge of the sheets (Figure S2 from Supporting Information) show several layers of unidirectionally aligned close-packed CdSe nanorods.

To reduce charging effect, we deposited the sheets of CdSe nanorods on ITO-coated glass. HRSEM imaging of the top surface of the sheets shows close-packed spherical projections consistent with the diameter of the nanorods. HRSEM images taken from the edge of a sheet fragment show a well-resolved superlattice of unidirectional aligned nanorods (Figures 3d and S3 from Supporting Information). CdSe nanorods self-assemble, forming layered structures where each layer consists of nanorods packed into long-range ordered hexagonal arrays. FFT analysis of a selected area (~240 nm × 240 nm) of HRSEM image confirms symmetry and length scale of ordering (insets in Figure 3d and Figure S3 from Supporting Information). This packing corresponds to smectic-B and crystalline phases. The nonzero size distribution of nanorod building blocks could lead to considerable disorder of crystalline phase superlattices in comparison with ordinary atomic, ionic, or molecular crystals. In Figure 3d, nanorods are seen stacked “one-on-one”, forming correlated vertical columns propagating through the layers. It is difficult to assign a specific space group to the nanorod superlattice because HRSEM does not allow us to determine the orientations of individual CdSe nanorods within the layers. Indeed, the wurtzite lattice of each CdSe nanorod lacks inversion symmetry, and top and bottom facets of CdSe nanorod, {001} and {00 $\bar{1}$ }, are intrinsically different (Figure 2b, inset).³³ Most probably, the 3D superlattice is stabilized by antiparallel dipole pairing within each layer and by head-to-tail pairing of nanorods from adjacent layers shown schematically in Figure 2b. This pairing would imply that self-assembly of CdSe nanorods may be driven by a combination of entropy and electrostatic forces.

Self-assembled CdSe nanorod solids exhibit specific birefringence. In a light microscope with crossed polarizers each spherical assembly shows a Maltese cross (Figure 4a). Moreover, in addition to the Maltese cross, concentric rings are seen along the radius at a higher magnification (Figure 4c). Similar birefringence has been observed for self-assembled CdSe nanorods with different sizes and aspect ratios. This effect is found only for the assemblies with the high degree of nanorod

(29) Li, L.-s.; Alivisatos, A. P. *Phys. Rev. Lett.* **2003**, *90*, 097402.

(30) McGrother, S. C.; Gil-Villegas, A.; Jackson, G. *Mol. Phys.* **1998**, *95*, 657.

(31) Dumestre, F.; Chaudret, B.; Amiens, C.; Respaud, M.; Fejes, P.; Renaud, P.; Zurcher, P. *Angew. Chem., Int. Ed.* **2003**, *42*, 5213.

(32) Shevchenko, E. V.; Talapin, D. V.; Kornowski, A.; Wieckhorst, F.; Kötzler, J.; Haase, M.; Rogach, A. L.; Weller, H. *Adv. Mater.* **2002**, *14*, 287.

(33) Shiang, J. J.; Kadavanich, A. V.; Grubbs, R. K.; Alivisatos A. P. *J. Phys. Chem.* **1995**, *99*, 17417.

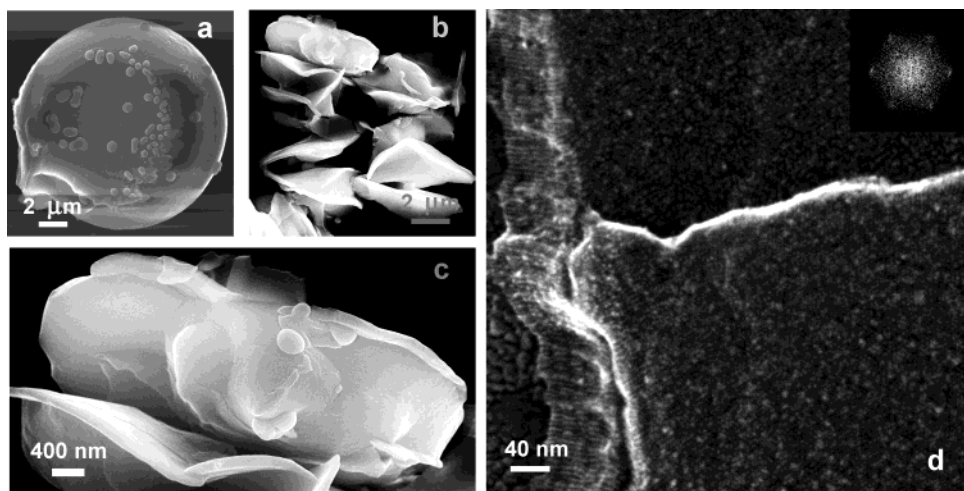


Figure 3. (a) SEM image of an assembly of $22 \text{ nm} \times 3.5 \text{ nm}$ CdSe nanorods. (b,c) Sonication of the nanorod assemblies results in their cleavage in several flat sheets. (d) High-resolution SEM image showing internal packing of CdSe nanorods inside the sheets. Vertical columns of nanorods at the edge of the superlattice show ordering in longitudinal direction. Inset: FFT from selected area of top surface of the nanorod sheet shown in frame (d) demonstrates hexagonal ordering of the nanorods within the layers. On the left, part of the image the ITO substrate can be seen.

ordering. The glassy films of CdSe nanorods prepared by fast deposition from a hexane solution exhibit neither Maltese crosses nor concentric rings (Figure 4d,e).

It is worth mentioning that similar polarized optical micrographs are observed for spherulite textures. Growth of a spherulite originates from a single nucleus (lamellae) followed by uniform growth in three dimensions to form ball-like structures.³⁴ In the case of a liquid crystal with spherulitic texture, the director rotates around the center of spherulite resulting in a crosslike extinction “Maltese cross”, which occurs along the polarization axes of the polarizers. Spherulites of polyethylene and some other polymers exhibit similar concentric extinction rings (radial banding) usually assigned to lamellar twisting along the radial direction during crystal growth.³⁵

The observed birefringence of nanorod assemblies can result from variations in the packing symmetry of nanorods across a platelet. The simultaneous appearance of Maltese crosses and concentric rings can be explained if the layer-by-layer growth results in a texture where smectically ordered layers are separated by ledges as shown in Figure 4f. In vicinity of the ledges, nanorods are tilted with respect to layer planes as shown in Figure 4f and rotate polarization of incident light. More detailed structural investigations are underway to understand textures and growth mechanism of CdSe nanorod superstructures.

Engineering the structure of the nanoscale building blocks and directing their self-assembly provide further options to design and optimize material properties. Our assembly technique is not limited to simple single-phase materials but can be extended to more sophisticated nanorod heterostructures. To demonstrate this, we have prepared ordered superstructures of CdSe/CdS heterostructure nanorods. These nanorods consist of a spherical CdSe core and CdS rod grown epitaxially on the $\{001\}$ facet of the CdSe core (Figure 5). The passivation of the spherical CdSe core with the elongated CdS shell results in efficient band gap photoluminescence (PL), which is linearly polarized along the nanorod. The room-temperature PL quantum

efficiencies exhibited by CdSe/CdS nanorods are 2 orders of magnitude higher than those of bare CdSe nanorods.²⁵ The CdSe/CdS heterostructure nanorods shown in Figure 5a,b can be self-assembled using the technique previously employed for assembling CdSe nanorods. Most of the CdSe/CdS nanorod superstructures appear in the optical microscope as flat semi-circles shown in Figure 5c. Figure 5e shows an SEM image of the nanorod assembly with more complex shape. The HRSEM image shown in Figure 5f shows spherical projections of individual nanorods hexagonally ordered inside a fragment of the CdSe/CdS nanorod superlattice. Self-assembled CdSe/CdS nanorod solids exhibit strong, stable PL under UV excitation (Figure 5d). We should note that the CdSe/CdS heterostructure nanorods are very efficient harvesters of short wavelength light because the CdS part provides large extinction below 500 nm (Figure S4 from Supporting Information). The carriers photo-generated in the CdS rod are efficiently captured in the CdSe core within $\sim 5 \text{ ps}$.²⁵ The CdSe/CdS heterostructure nanorods emit in the spectral region where only the CdSe core can reabsorb the emitted light (Figure S4 from Supporting Information). The extinction coefficients in this spectral region are relatively small. This means that reabsorption in CdSe/CdS heterostructure nanorod solids is considerably smaller than reabsorption in CdSe or any other single-phase nanorod solids. This makes CdSe/CdS nanorods particularly interesting for solid-state luminescence applications such as phosphors, light-emitting diodes and lasers, as well as for detectors and for light harvesting applications. Engineering the shell of organic capping ligands (e.g., the use of functionalized oligothiophenes proposed in ref 36) in combination with the nanorod alignment perpendicular to a substrate should result in significant improvement of performance of nanorod-based hybrid solar cell.³⁷

In summary, we have, for the first time, observed the organization of semiconductor nanorods into ordered 3D superstructures. The proposed self-assembly technique is shown to be applicable to a range of nanorod materials. These artificial

(34) Phillips, P. J. In *Handbook of Crystal Growth*; Hurlte, D. T. J., Ed.; North-Holland: Amsterdam, 1994.

(35) Singfield, K. L.; Hobbs, J. K.; Keller, A. *J. Cryst. Growth* **1998**, *183*, 683.

(36) Milliron, D. J.; Alivisatos, A. P.; Pitois, C.; Edler, C.; Fréchet, J. M. J. *Adv. Mater.* **2003**, *15*, 58.

(37) Huynh, W. U.; Dittmer, J. J.; Alivisatos, A. P. *Science* **2002**, *295*, 2425.

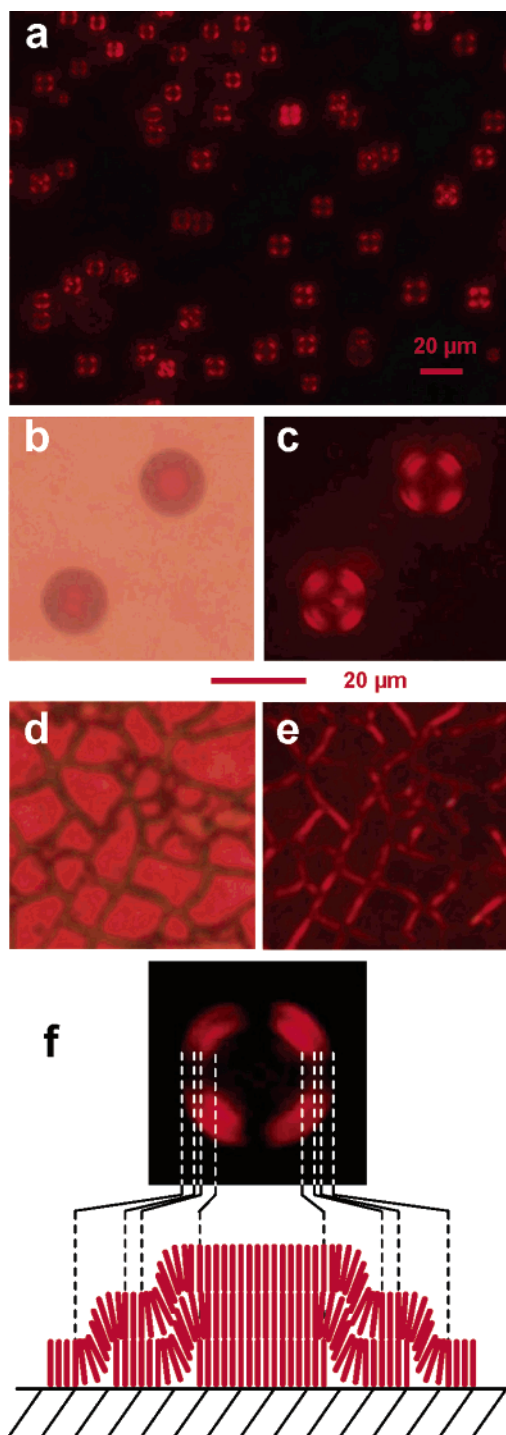


Figure 4. (a) Optical micrograph of assemblies of $22 \text{ nm} \times 3.5 \text{ nm}$ CdSe nanorods viewed between crossed polarizers. (b,c) Optical micrographs of self-assembled nanorods observed without (b) and with (c) crossed polarizers at higher magnification. (d,e) Optical micrographs of a glassy film of CdSe nanorods observed without (d) and with (e) crossed polarizers. (f) Scheme showing a possible packing of nanorods in the assemblies that is consistent with simultaneous appearance of Maltese crosses and concentric rings.

nanorod solids display strong optical anisotropy and are expected to exhibit anisotropic electrical and mechanical properties arising from both the intrinsic anisotropy of the building blocks and the collective physical properties of the superlattice.

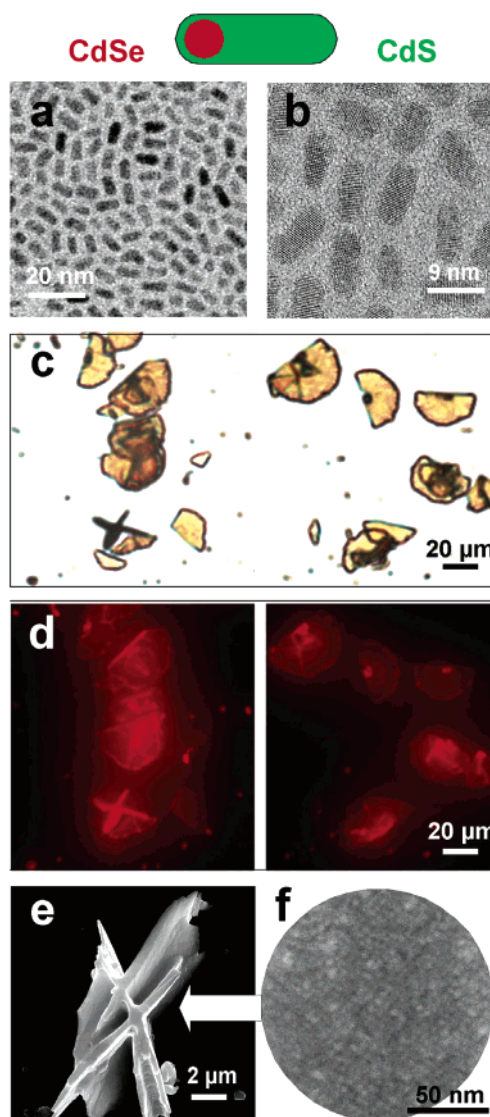


Figure 5. (a) TEM and (b) HRTEM images of CdSe/CdS heterostructure nanorods with the internal structure sketched on top of the figure. (c) Optical micrograph of self-assembled superstructures of CdSe/CdS nanorods. (d) CdSe/CdS nanorod solids exhibit bright and stable PL under UV excitation. (e) SEM image of the self-assembled colloidal crystal built from CdSe/CdS nanorods. (f) HRSEM image of the colloidal crystal surface shown in frame (e). CdSe/CdS nanorods are seen ordered into a superlattice.

Acknowledgment. We thank Sylvia Bartholdi-Nawrath for help with TEM and HRSEM investigations, Uwe Borchert and Maren Krack for help with optical microscopy, and Prof. V. Vill for helpful discussions. This work was supported by Deutsche Forschungsgemeinschaft through SFB 508 and NATO Scientific and Environmental Affairs Division.

Supporting Information Available: TEM image of the CdSe nanorod assembly with nematic ordering (Figure S1). High-resolution SEM images of CdSe nanorod solids (Figures S2 and S3). UV-vis and PL spectra of CdSe/CdS heterostructure nanorods (Figure S4). This material is available free of charge via the Internet at <http://pubs.acs.org>.

JA046727V